Mol Neurobiol (2012) 46:304–315
DOI 10.1007/s12035-012-8288-3

Glucocorticoid Receptors are Localized to Dendritic Spines and Influence Local Actin Signaling

Matiar Jafari · Ronald R. Seese · Alex H. Babayan · Christine M. Gall · Julie C. Lauterborn

Received: 9 April 2012 / Accepted: 5 June 2012 / Published online: 21 June 2012

Abstract Glucocorticoids affect learning and memory but the cellular mechanisms involved are poorly understood. The present studies tested if the stress-responsive glucocorticoid receptor (GR) is present and regulated within dendritic spines, and influences local signaling to the actin cytoskeleton. In hippocampal field CA1, 13 % of synapses contained GR-immunoreactivity. Three-dimensional reconstructions of CA1 dendrites showed that GR aggregates are present in both spine heads and necks. Consonant with evidence that GRα mRNA associates with the translation regulator Fragile X Mental Retardation Protein (FMRP), spine GR levels were rapidly increased by group 1 mGluR activation and reduced in mice lacking FMRP. Treatment of cultured hippocampal slices with the GR agonist dexamethasone rapidly (15–30 min) increased total levels of phosphorylated (p) Cofilin and extracellular signal-regulated kinase (ERK) 1/2, proteins that regulate actin polymerization and stability. Dexamethasone treatment of adult hippocampal slices also increased numbers of PSD95+ spines containing pERK1/2, but reduced numbers of pCofilin-immunoreactive spines. Dexamethasone-induced increases in synaptic pERK1/2 were blocked by the GR antagonist RU-486. These results demonstrate that GRs are present in hippocampal spines where they mediate acute glucocorticoid effects on local spine signaling. Through effects on these actin regulatory pathways, GRs are positioned to exert acute effects on synaptic plasticity.

M. Jafari · R. R. Seese · A. H. Babayan · J. C. Lauterborn (✉)
Department of Anatomy and Neurobiology, 3226 Gillespie Neuroscience Research Facility, University of California at Irvine, Irvine, CA 92697-1275, USA
e-mail: jclauter@uci.edu

C. M. Gall
Department of Anatomy and Neurobiology, 3123 Gillespie Neuroscience Research Facility, University of California at Irvine, Irvine, CA 92697-1275, USA

Keywords Dexamethasone · Extracellular signal-regulated kinase · Fragile X Mental Retardation Protein · Cofilin · Rho GTPase · Glucocorticoid receptor

Introduction

Glucocorticoids exert a wide range of effects on hippocampal neurons including regulating gene expression, cell survival, AMPA receptor cycling, dendritic morphology, and synaptic plasticity [1–3]. While many of these effects depend upon changes in gene expression and require some time to occur (i.e., >15–30 min), there is mounting evidence that the hormone also has rapid, non-genomic actions [4, 5] such as the modulation of Ca^{2+} currents [6], glutamatergic transmission [7], and p38 MAPK signaling [8].

Corticosterone, the glucocorticoid in rodent, acts on both mineralocorticoid and glucocorticoid receptors (GRs), in concentration-dependent fashions. Genomic effects of the steroid are mediated by receptors in the cytosol, whereas non-genomic actions are thought to occur via interactions with membrane-bound receptors and involve G protein-dependent mechanisms and downstream kinases ([9] for review). Although GRs have been localized to neuronal cell bodies and dendrites, few studies have examined the synaptic localization of this receptor. Johnson et al. [10] found GRs are present in dendritic spines in the lateral amygdala, whereas Komatsuzaki et al. [11] identified GRs in hippocampal synaptosomal fractions. Although the latter would include dendritic spines, in addition to presynaptic elements, definitive evidence for spine localization of the GRs in hippocampus is lacking. A recent study identified GRα mRNA as a target of the local translation regulatory protein FMRP [12] suggesting that, within spines, GR levels may be regulated by local protein synthesis, but this has yet to be

examined. Ultimately, more information on the localization and regulation of GRs in hippocampal dendritic spines is needed to understand how this receptor exerts its complex effects on synapse function and enduring synaptic plasticity in this structure [13].

Evidence that glucocorticoids can suppress hippocampal long term potentiation (LTP) [14–17] suggests that the hormone may act locally through GR receptors on dendritic spines to influence mechanisms of plasticity. Activity-dependent remodeling of the dendritic spine actin cytoskeleton is now appreciated to be critical for enduring LTP in hippocampus [18–20]. In non-neural cells, glucocorticoids modulate actin networks via signaling through the Rho GTPases RhoA [21, 22] and Rac [23]. These same cascades are activated in dendritic spines with induction of LTP and are critical for local, activity-induced increases in the polymerization and stabilization of F-actin [19, 30], but the proximity of the GRs to these events and the influence of glucocorticoids on spine actin remodeling in mature neurons are not known.

The present study addressed these issues and, specifically, for hippocampal field CA1 examined the localization and regulation of GR in dendritic spines, and the mechanisms by which glucocorticoids influence the spine actin cytoskeleton. We find GR aggregates are indeed present within pyramidal cell dendritic spines and that receptor levels are regulated by group 1 mGluR activation, suggesting that activity regulates GR levels at glutamatergic synapses. Additionally, we demonstrate that via the GRs, glucocorticoids engage signaling pathways that regulate spine actin networks.

Materials and Methods

Animals and Tissue Preparation

Unless otherwise stated, studies used adult (2–4 months old) male Sprague-Dawley rats or C57BL/6 mice. Some experiments examined effects of the absence of FMRP on GR content; these used adult (3-month-old) male C57BL/6 *Fmr*1 knockout and wild-type mice [24]. Analyses of immunolabeling within specific dendritic compartments employed adult male mice that express enhanced green fluorescent protein (GFP) under control of the Thy-1 promoter in scattered CA1 hippocampal neurons (i.e., line M of [25]). Because levels of circulating corticosterone follow a circadian rhythm with concentrations being lowest at the beginning of the light cycle and rising to maximal levels at the beginning of the dark cycle [26], all animals were killed between 9 and 10 A.M. early in the light cycle (starts 6 A.M.). To mitigate the potential for stress at time of sacrifice, animals were rapidly (within 2–3 min) anesthetized and killed. Efforts were made to minimize numbers of animals used, and all procedures were conducted in accordance with NIH guidelines and were approved by the Institutional Animal Care and Use Committee.

For immunofluorescence studies, animals were killed by isoflurane anesthesia and decapitation. Brains were removed, frozen by immersion into −50 °C 2-methylbutane and cryostat sectioned (20 μm, coronal plane) through hippocampus. Spaced series of sections were collected onto Superfrost slides (Fisher Scientific), fixed in −20 °C methanol for 20 min, rinsed in 0.1 M phosphate buffer, pH 7.2 (PB), air-dried, and stored at −20 °C until use. For studies using GFP-expressing mice, animals were perfused with 4 % paraformaldehyde in PB; brains were postfixed overnight and then cryoprotected in 30 % sucrose in 4 % paraformaldehyde. Tissue was sectioned on a freezing microtome through the septal third of hippocampus (30 μm, coronal) and a spaced series was collected into 0.1 M PB for immunofluorescence analysis.

Acute Hippocampal Slices

Transverse hippocampal slices (350 μm thick) were prepared from 1 month old male rats as described [19]. Slices were cut into ice-cold artificial cerebrospinal fluid (ACSF; in mM: 124 NaCl, 3 KCl, 1.25 KH_2PO_4, 2.5 $CaCl_2$, 1.5 $MgSO_4$, 26 $NaHCO_3$, and 10 dextrose, pH 7.4), distributed across two interface recording chambers and maintained at 31±1 °C with the upper surface exposed to humidified 95 % O_2/5 % CO_2; ACSF was constantly perfused at a rate of 60–70 ml/h. Slices equilibrated in the chamber for 2 h before treatment. Dexamethasone (DEX) was added to the tissue bath via a second perfusion line to attain a final 5 μM concentration; slices were treated for 5, 15, or 30 min as indicated in the experimental results. Control slices received vehicle-ACSF treatment and were collected at 30 min; this time point was selected because preliminary studies indicated no difference in immunostaining between 5 and 30 min vehicle-controls. Immediately following treatment, slices were collected into cold 4 % paraformaldehyde and fixed overnight (4 °C) prior to sectioning (25 μm) and processing for double immunolabeling.

Double-Labeling Immunofluorescence

Tissue was processed for dual immunofluorescence as described [19, 27]. A rabbit antiserum directed against the N terminus of mouse GR (M20; 1:400; #sc-1104, Santa Cruz), which recognizes both GRα and GRß subunits, was used. The M20 antibody was chosen for the present work because it has been shown to have greater specificity for cytoplasmic, as opposed to nuclear, GR in rat hippocampal cells as compared to other antibodies [28]. The anti-GR antibody was used in combination with mouse antisera to the post-

synaptic density (PSD) protein PSD95 (1:1,000; #1-054 Affinity BioReagents/Thermo Fisher Scientific), the lipid raft component flotillin (1:200, #610802, BD Biosciences) [29], or the synaptic vesicle protein synaptophysin (1:1,000, #S5768, Sigma-Aldrich). For other studies, a cocktail of either rabbit anti-phosphorylated (p-) Cofilin Ser3 (1:100; #ab12866, Abcam) or rabbit anti-pERK1/2 Thr202/Tyr204 (1:500, #4370, Cell Signaling) in combination with mouse anti-PSD95 (1:1,000; #1-054) was used. Tissue was incubated in the primary antisera cocktail overnight, rinsed in PB, and then incubated in a secondary antisera cocktail containing anti-mouse Alexafluor-488 and anti-rabbit Alexafluor-594 (1:1,000 each, Invitrogen) for 1 h. The diluent for both primary and secondary incubations was PB containing 4 % BSA and 0.3 % Triton X-100, and incubations were conducted at room temperature. Following final washes in PB, the tissue was coverslipped with Vectashield containing DAPI (Vector Labs).

Analysis of Double Immunolabeling

Analysis of immunofluorescence double-labeling in stratum (str.) radiatum of hippocampal field CA1 was conducted as previously described in numerous studies [19, 30–34]. The studies focused on field CA1 because glucocorticoids have been shown to influence both spine measures [11, 35, 36] and LTP [15, 16, 37, 38] in CA1 and, among the hippocampal subfields, activity-induced signaling to spine filamentous (F-) actin has been most extensively studied [19]. Image Z-stacks of the 105×136 μm sample field were collected through a depth of 3 μm at 0.2 μm steps (42,840 μm^3 total sample field size) using a Leica DM6000 epifluorescence microscope with a 63× objective. For analysis of brain tissue sections, approximately 15 image stacks were collected from 6 to 8 sections per brain for each antisera combination. For analysis of hippocampal slices, 10 image stacks from 5 tissue sections were evaluated. Image stacks were processed for iterative deconvolution (Volocity 4.1; Perkin Elmer) and then in-house software was used to construct three-dimensional (3D) montages and to quantify double-labeled (e.g., both GR- and PSD95-immunoreactive) or single-labeled puncta as detailed in Rex et al. [19] and Chen et al. [30–32]; these earlier studies from our laboratory used the protocol for identifying and assessing specific proteins of interest in PSD95-immunopositive spines. Briefly, image *Z*-planes were normalized to 30 % of maximum background intensity and iteratively binarized at regular intensity thresholds using exclusion criteria for object size and ellipticity (optimized for spine detection), followed by dilation and erosion filtering. Repeated observations were binned and analyzed to assess object boundaries and to discriminate neighboring objects; this process accurately identifies both faintly and densely labeled objects. Finally, objects were reconstructed in 3D to calculate volume and position. For each image Z-stack, both immunolabels were evaluated independently and labeled objects were considered colocalized if any of their boundaries overlapped as evaluated in 3D. Counts of single- and double-labeled puncta across tissue sections were averaged to produce individual animal or hippocampal slice means that were then averaged to generate the group mean±SEM values presented in the text and figures.

Confocal Microscopy and 3D Reconstructions in GFP-Expressing Mice

Tissue sections through hippocampus were processed for dual immunolabeling using rabbit anti-GR (1:400; #sc-1104) and chicken anti-GFP (1:1,000; #ab13970, Abcam) followed by secondary incubation in anti-chicken Alexafluor-488 and anti-rabbit Alexafluor-594 (1:1,000) as described above. After final PB rinses, the sections were slide-mounted and coverslipped with Vectashield. Immunohistochemical labeling of GPF was used to enhance visualization of the fluorophore in spine necks.

Image Z-stacks were collected using a Zeiss 710 confocal microscope at Nyquist rate with a 63× objective. Lasers were set at 488 and 561 excitation wavelengths to optimally visualize the two emissions while excluding overlap and, thus, bleed through. Images of GFP-labeled secondary dendrites of CA1 pyramidal neurons were collected at 0.13 μm focal steps through the entire depth of each dendrite. Seven dendrites from three mice were evaluated for each of three mice. The image stacks were deconvolved for 10 iterations using AutoQuant (v2.10; MediaCybernetics) and 3D renderings of the dendrites were made using Imaris (v7.1.0; Bitplane Inc.). Builds of the GFP-labeled dendrites were used as a mask for the red (GR) channel, and all red labeling not encompassed by the dendritic build was eliminated. For quantification, a volumetric build was created for all red intensities and then counts of these labeled profiles in spine heads and necks were conducted manually.

Cultured Hippocampal Slices

Hippocampal slice cultures were prepared from postnatal day (P) 8–9 Sprague-Dawley rat pups of both sexes and explanted onto Millipore culture inserts as described [34]. Slices were maintained in culture at 37 °C with 5 % CO_2 for 10–12 days in medium containing 20 % horse serum (pH 7.2). The day before treatment, the cultures were transferred to serum-free medium. The cultures were treated with 5 μM DEX in serum-free medium for 15 min to 1 h, and immediately collected into frozen microcentrifuge tubes for subsequent protein measures by western blotting. At treatment, the DEX-containing medium was briefly (~10 s) washed over the cultures and then moved by pipette to the bottom of the tissue culture well for the duration of the

treatment period. For controls, tissue was similarly treated with serum-free medium.

Synaptoneurosomes

Male and female P18–21 Sprague-Dawley rats were used to prepare synaptoneurosomes (SNS) using the ficoll gradient technique as described in detail elsewhere [39]. Sample protein contents were adjusted to 1.5 μg/μl before treatment of SNS aliquots with 20 μM (RS)-3,5-dihydroxyphenylglycine (DHPG) or ACSF for 5 min, or with ACSF or RU-486 (1 μM) for 5 min followed by DEX (5 μM) for 5 min. Treatments were terminated by addition of 5× gel loading buffer and then samples were boiled at 100 °C for 5 min, briefly placed on ice, and stored at −80 °C until processed for western analyses.

Western Blot Analyses

Tissue was homogenized and processed for western blots as previously described [39]. Proteins were separated by 10–12 % PAGE and transferred to PVDF membranes (Amersham). The membranes were incubated overnight at 4 °C, or at room temperature for 2 h, with the following primary antibodies: rabbit anti-p-Cofilin Ser3 (1:2,000; #ab12886, Abcam), rabbit anti-p-PAK1,2,3 Thr423 (1:2,000; #2601, Cell Signaling), rabbit anti-p-PAK1,2,3 Ser141 (1:10,000; #44-940G, Invitrogen), mouse anti-p-ERK1/2 Thr202/Tyr204 (1:2,000; #9106, Cell Signaling), rabbit anti-GR (1:1,000; Santa Cruz), and mouse anti-actin (1:10,000; A1978, Sigma-Aldrich).

Statistical Analyses

For comparison of two groups the Student's t test was used. For comparison of three or more groups, a one-way ANOVA was performed followed by either Student–Newman–Keuls (SNK) or Tukey's test for post hoc comparisons; results of post hoc tests are given in figures where appropriate. For all cases, $p<0.05$ was considered significant.

Results

GR Localization to Pyramidal Cell Spine Synapses

In rat hippocampal field CA1, GR immunolabeling was localized to granules both within the pyramidal cell perikarya and rather evenly distributed across the dendritic fields. Because previous reports have shown an enrichment of GRs in the septal pole of hippocampus [16], the possibility of GR localization at excitatory spine synapses was assessed in sections through rostral hippocampus and, specifically, within the apical, stratum radiatum of field CA1. Tissue sections were processed for dual immunofluorescence localization of GR and the excitatory synapse scaffold protein PSD95; in CA1 str. radiatum PSD95 is concentrated exclusively at excitatory spine synapses [40, 41]. As shown in Fig. 1a (left), both single-labeled and double-labeled puncta were observed. Counts of labeled elements within the size constraints of synaptic components revealed that of the GR-immunopositive (+) puncta, 36±6 % were colocalized with PSD95 (Fig. 1a, right) thereby indicating that a substantial portion of the receptor pool is present in the postsynaptic compartment of excitatory synapses. Of the PSD95+ synapses, 13±2 % contained GR-immunoreactivity (ir).

Similar analysis of GR localization in sections through C57BL/6 mouse hippocampus demonstrated that, in these animals, 15±1 % of PDS95+ synapses contained GR-ir whereas 15±4 % of GR+ puncta were colocalized with PSD95.

To assess the degree to which GRs are localized to presynaptic elements and lipid rafts, tissue sections through rat hippocampus were evaluated for the colocalization of GR with synaptophysin and flotillin, respectively. Of the GR+ puncta in CA1 str. radiatum, 19±5 % were synaptophysin+ and 28±4 % were flotillin+ indicating rather comparable GR distribution across the three cellular compartments evaluated.

Localization of Dendritic GR-ir in GFP-Expressing Hippocampal Neurons

PSD95 is concentrated at spine synapses in field CA1 [42, 43]. Thus, the colocalization of GR and PSD95 (above) indicates that the GRs are, at least in part, localized to spines in hippocampus proper. To verify this, tissue from Thy1-GFPm mice, which express GFP in scattered hippocampal pyramidal neurons under control of the Thy-1 promoter [25], was processed for dual (GFP/GR) immunofluorescence and 3D reconstruction of immunolabeled secondary dendrites in field CA1. Confocal image Z-stacks were collected of GFP-labeled dendrites (green) containing anti-GR labeled elements (red), and 3D builds were generated (Fig. 1b–f). As shown in Fig. 1g–k, GR+ puncta were distributed to both the shafts and spines of labeled dendrites. Within spines, the placement of GR+ puncta varied but included some situated at the tip of the spine head (Fig. 1g, i) and others along the sides of the spines (Fig. 1h). Occasionally, GR+ puncta were localized within spine necks (Fig. 1j, asterisk). The number of GR+ puncta contained within spines for seven separate dendritic builds (each 50 μm long) were quantified. Of the 1041 spines, 169 had GR+ puncta in the heads; this represented 16.0±2.9 % of the total spines per dendritic span evaluated and is consistent with the GR/PSD95 colocalization result (Fig. 1a). Further, 87 of the spines (9.9±3.1 % of spines per dendrite) had GR+ puncta in their necks; the association of these GR+

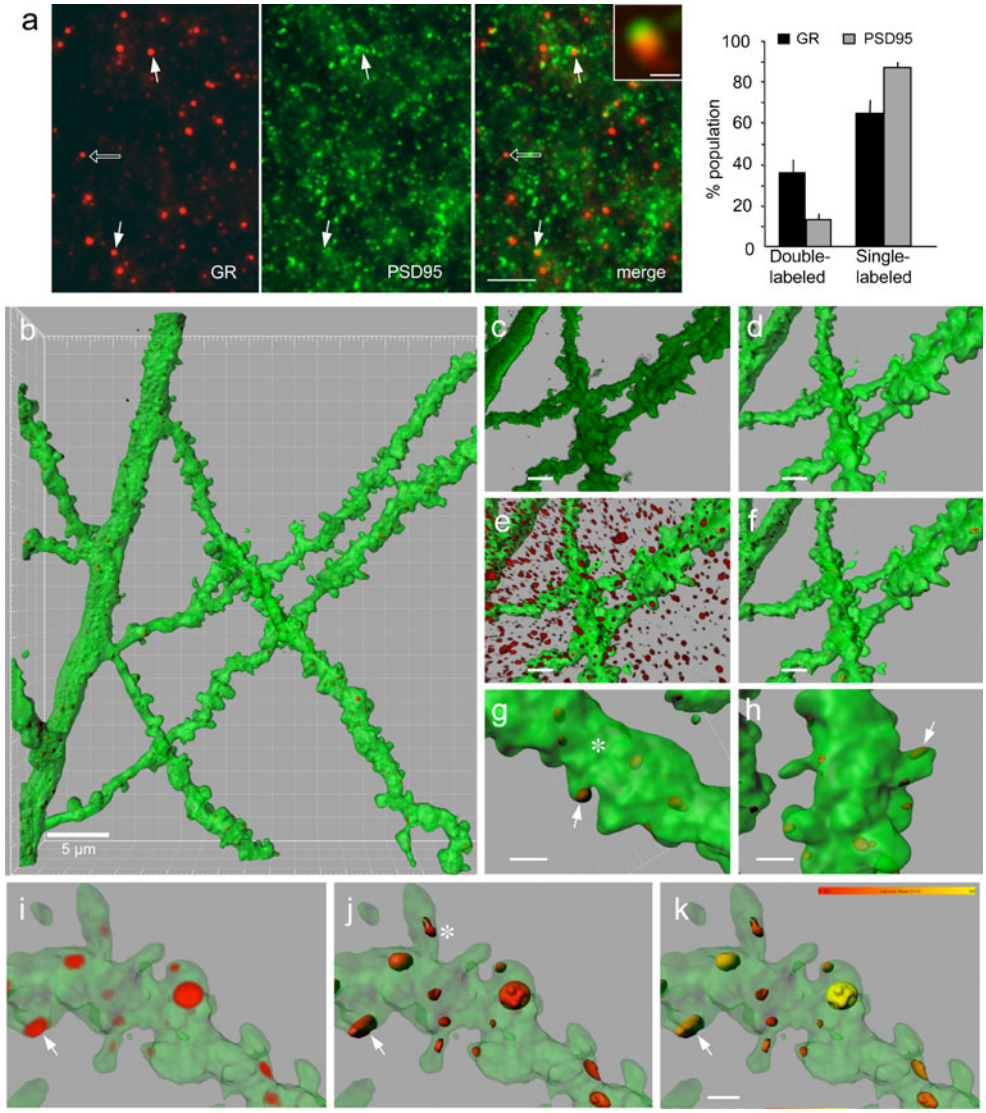

Fig. 1 Glucocorticoid receptor (GR) aggregates are localized to dendritic spines. **a** *Left* Deconvolved, wide-field images of rat CA1 str. radiatum show immunolabeling for GR (*left*; *red*), PSD95 (*middle*; *green*), and a "merge" of the two (*right*). Both single-labeled (*open arrow*) and double-labeled (*filled arrowheads*) puncta are observed (*bar*=10 μm); *inset* shows one double-labeled element (*bar*= 0.5 μm). *Right* Bar graph shows quantification of single- and double-labeled puncta expressed as percent of the total population of elements labeled for the same antigen (mean±SEM values; *n*=5 brains). **b–k** Dual immunofluorescence and 3D renderings of elements within confocal image Z-stacks that were used to localize GR-immunoreactivity (ir) (*red*) in GFP-labeled dendrites (*green*) of mouse CA1 pyramidal cells (str. radiatum). **b** Rendering of multiple GFP-labeled dendrites shows that small GR-immunopositive (+) puncta are broadly but sparsely scattered throughout (*bar*=5 μm). **c–f** Images show stages in the process by which GR immunolabeling was visualized. Using Imaris software, the *green channel* showing GFP labeling (**c**) was first processed for 3D rendering (**d**). The 3D build was then used as a mask for the *red channel* (**e**) and all red not encompassed by the build was digitally removed for easier visualization of GR-ir within GFP-labeled structures (**f**; *bars*=2 μm). **g**, **h** High magnification images show examples of spines on secondary dendrites that contained GR+ puncta (*arrows*): the GR+ patches are present both at the head (**g**, *arrow*) and along the sides (**h**, *arrow*) of spines, as well as within the dendritic shaft (**g**, *asterisk*; *bars*=1 μm). **i–k** 3D builds of a secondary dendrite containing GR+ puncta in spines and the dendritic shaft. In **j**, the image of the GFP-labeled dendrite was made semi-transparent to allow for better visualization of GR+ puncta within its depth; *arrow* shows a large GR+ element positioned at the spine surface. Note the presence of puncta in spine necks (*asterisk*). In **k**, color-coding of GR-immunofluorescence intensity (*red*=lower, *yellow*=higher; see *bar* at *upper right*) shows that the larger puncta have greater immunolabeling (*bar*=0.5 μm)

clusters with postsynaptic elements was likely not detected in the GR/PSD95 colocalization analysis (described above) because of the physical separation between PSD95-ir at the synaptic active zone and the GR-ir in the spine neck. Finally, less than 2 % of all spines analyzed contained more than one GR-immunoreactive puncta. Together, counts from the 3D builds demonstrate that 23.9±2.6 % of the spines on CA1 pyramidal cell secondary dendrites contain GR aggregates.

Group 1 mGluR Activation Increases GR Content in Synaptoneurosomes

Recent work suggests that GRα mRNA may be cargo of FMRP [12], a regulator of group 1 mGluR-dependent local protein synthesis in spines [44]. Accordingly, we tested the prediction that group 1 mGluR stimulation would influence synaptic GR content using rat synaptoneurosomes (SNS), a preparation enriched in both pre- and postsynaptic elements [39]. Treatment of SNS with the group 1 agonist (RS)-3,5-dihydroxyphenylglycine (DHPG; 20 μM) for 5 min caused a 30±6 % increase in GR-ir relative to yoked vehicle-treated control SNS ($p<0.0423$, Student's t test, Fig. 2a) as determined by western blots (normalized to sample actin levels). These results indicate that GR protein is synthesized in spines in response to mGluR stimulation and, thus, in response to synaptic activity.

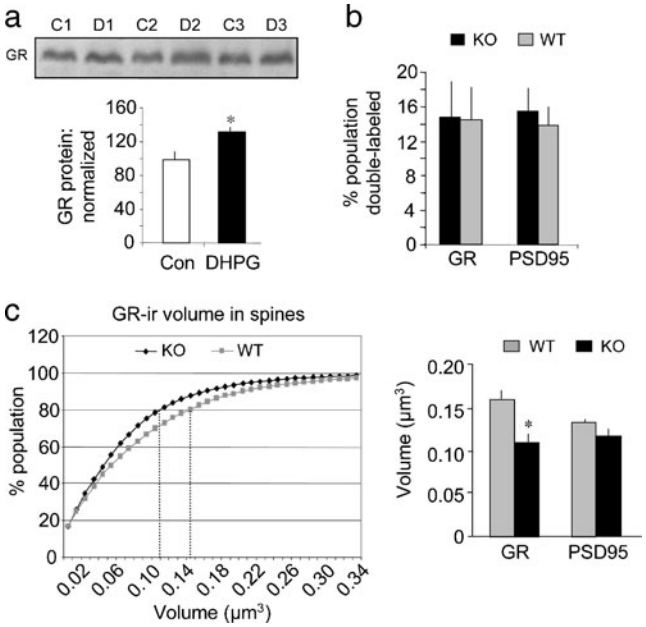

Fig. 2 Spine GR levels are regulated by group 1 mGluRs and reduced in Fmr1-KOs. **a** At the *top*, western blot analyses shows GR-immunoreactivity in rat synaptoneurosomes treated (5 min) with the group 1 mGluR agonist DHPG ("D") and their corresponding vehicle-controls ("C"). *Below*, plot shows quantification of GR-immunoreactivity (normalized to actin; $n=4$/group): 5 min of DHPG treatment significantly increased GR content (*$p=0.0423$, Student's t test). **b** Bar graph shows quantification of double-immunolabeled (GR/PSD95) puncta in CA1 str. radiatum of Fmr1-KO (KO) and wild-type (WT) mice ($n=3$/genotype): counts are expressed as percent of either total GR-immunopositive (+) or total PSD95+ puncta. As shown, there was no difference in numbers of GR+ spines between genotypes. **c** Cumulative frequency distributions for volumes (μm^3) of GR-ir puncta localized to PSD95+ spine synapses (*left plot*). As shown, the GR+ puncta size distribution is shifted to the left in KO as compared to WT spines, denoting smaller GR aggregates in the mutants. *Right plot* shows individual animal means at the 80th percentile for GR+ and PSD95+ elements in double-labeled spines: volumes of GR+ puncta were significantly smaller in KOs vs WTs (*$p=0.03$, Student's t test), whereas volumes of PSD95-ir puncta, for the same spines, did not differ between genotypes

FMRP Expression Influences Spine GR Levels

In addition to regulating local protein synthesis, FMRP is involved in the transport of mRNAs into dendrites and spines [45, 46]. In mice lacking FMRP expression, due to a knockout of the *Fmr1* gene (i.e., Fmr1-KO), GR-ir in dendrites of hippocampal CA1 neurons is reportedly concentrated near the cell bodies suggesting that normal GR distributions depend on FMRP-transport functions [12]. Accordingly, we tested if the association of GR with PSD95+ excitatory synapses is disturbed in hippocampus of Fmr1-KO mice (although PSD95 translation is in part regulated by FMRP [47], previous work found no difference in the number of PSD95+ synapses in CA1 str. radiatum of Fmr1-KO and wild-type mice [30]). As shown in Fig. 2b, we found no difference in the association of GR-ir with PSD95+ elements in CA1 str. radiatum of Fmr1-KOs and wild-type mice: about 15 % of the PSD95+ synapses was associated with GR-ir in both genotypes. Moreover, of the GR+ puncta, about 15 % was double-labeled for PSD95 in both genotypes; it should be noted that the proportion of GR+ elements colocalized with PSD95 in CA1 str. radiatum differs between mice (~15 %) and rats (over 30 %).

Next, we examined the volumes of GR+ puncta that were colocalized with PSD95 in CA1 str. radiatum of Fmr1-KO and WT mice. As shown in cumulative volume distributions presented in Fig. 2c, the GR+ elements associated with PSD95 were smaller (i.e., volume distributions were shifted to the left) in Fmr1-KO as compared to WT tissue. By contrast, the volume distributions of PSD95+ puncta (both single- and double-labeled) in these same sample fields did not differ between genotypes ($p>0.05$). Notably, the GR-ir puncta *not* associated with PSD95 exhibited no volumetric differences between genotypes. These data suggest that while the numbers of PSD95+ spine synapses associated GR is not influenced by FMRP, the GR content of those spines reflects the presence of FMRP and is abnormally low in its absence.

Glucocorticoid-Mediated Signaling to Actin Regulatory Proteins

Glucocorticoids are known to affect the actin cytoskeleton in diverse non-neuronal cell types, but little is known about the degree to which this occurs in neurons or the mechanisms involved. This possibility is of particular interest regarding the spine actin cytoskeleton as recent studies have shown that spine actin remodeling is critical for the stabilization of hippocampal LTP and hippocampus-dependent memory formation [20, 27, 33, 48], two processes that are

modulated by stress and GR stimulation [13, 49]. We evaluated the effects of the synthetic glucocorticoid DEX on activation of several actin regulatory proteins first using cultured hippocampal slices and western blotting to gain insights into the general effects of this hormone on the target proteins. Slices were prepared from P8-9 rat pups and treated with DEX after 10–12 days in vitro; whole slice homogenates were then evaluated for treatment effects on levels of phosphorylated cofilin Ser3, p21-activated kinase (PAK) Ser141, and extracellular signal-regulated kinase 1/2 (ERK1/2; a.k.a. p44/42 MAPK) Thr202/Tyr204. The actin severing protein cofilin is inactivated by Ser3 phosphorylation thereby allowing further elongation of polymerizing actin filaments [50]. PAK is a downstream effector of the Rho GTPase Rac1 and is involved in F-actin stabilization through effects on downstream proteins (see [27]). PAK is activated by phosphorylation at Ser141 and then Thr423; the phospho-specific antisera to PAK used here recognize conserved sites in PAKs 1–3. The serine kinase ERK1/2 regulates activities of the cortactin/Arp2/3 complex and, thereby, F-actin stabilization and branching [51–53], and ERK1/2 has been shown to positively regulate actin polymerization in supraoptic neurons [54]. All three signaling markers (cofilin, PAK, ERK) are implicated in activity-induced spine actin remodeling and LTP [19, 27, 55, 56].

DEX treatment induced a marked increase in pCofilin in whole slice homogenates that was evident at 15 min and significant from 30 min to 1 h of treatment (Fig. 3a, b). DEX more modestly increased pERK1/2 at 15 and 30 min with levels returning to control values by 1 h (Fig. 3a, c), but had no detectable effects on pPAK Thr423 (Fig. 3b) or pPAK S141 (not shown).

These results indicate that glucocorticoids engage actin regulatory pathways in hippocampus but do not address the extent to which this occurs in dendritic spines. Therefore, to further interrogate glucocorticoid actions on actin regulation in spines, the effects of DEX on the same signaling proteins were evaluated in synaptoneurosomal preparations. As shown in Fig. 4a, a 5-min DEX treatment increased SNS pERK1/2 levels by 62 % as compared to vehicle-controls ($p<0.001$, Tukey's); this increase was rapidly transient and had fully dissipated in samples collected 15 or 30 min after treatment onset. The effect of DEX on pERK1/2 was blocked by pretreatment with the GR antagonist RU-486 ($p=0.1635$ vs control, t test) verifying that it was indeed mediated by GRs (Fig. 4b). DEX had no effect on SNS levels of pPAK Ser141 or pCofilin at any time point examined (Fig. 4a).

Because ERK1/2 is localized to both presynaptic and postsynaptic elements, and work has shown that mineralocorticoid receptors activate ERK1/2 in the presynaptic compartment [57], we further tested the effect of DEX on spine pERK1/2 levels using adult rat hippocampal slices and dual-immunofluorescence localization of pERK1/2 Thr202/Tyr204 and PSD95 (Fig. 5a); labeled puncta were quantified in CA1 str. radiatum. As shown in Fig. 5b, 5 μM DEX treatment significantly increased numbers of PSD95+ puncta containing pERK1/2 at 5 min; this timing is consistent with the results obtained in SNS (Fig. 4a). At 15 and 30 min, numbers of doubled-labeled puncta were not significantly different from controls.

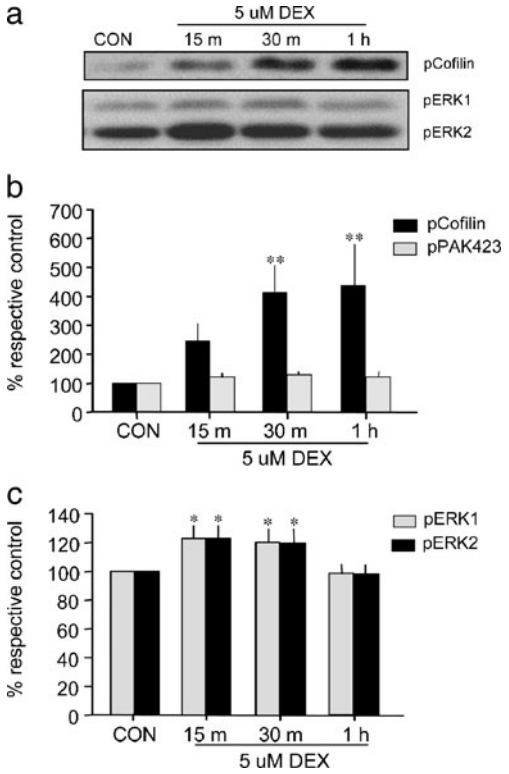

Fig. 3 DEX increases phosphorylation of cofilin and ERK1/2. **a** Representative western blots show effects of 5 μM DEX treatment for 5 min, 30 min, or 1 h on levels of phosphorylated (p) Cofilin Ser3 and pERK1/2 Thr202/Tyr204 in cultured hippocampal slices as assessed from whole slice homogenates. **b**, **c** Quantification of DEX treatment effects on pCofilin and pPAK1,2,3 Thr423 (**b**), and on pERK1/2 (**c**) levels; measures of western blot band densities were normalized to actin content (for the same blot and lane) and were then expressed as percent of paired control values. As shown, DEX treatment increased levels of pCofilin and pERK but had no effect on pPAK (*$p<0.05$; **$p<0.01$ vs control, SNK post hoc test; $n=15$/group)

The disparity between the effects of DEX on pCofilin levels in whole hippocampal slice homogenates (an increase) and SNS (no effect) led us to test if DEX influences pCofilin levels in spines in situ (as opposed to within the reduced SNS preparation). Adult rat hippocampal slices were treated with 5 μM DEX for 5, 15, or 30 min, processed for immunofluorescence, and the number of PSD95+ elements associated with pCofilin-ir in CA1 str. radiatum was quantified. As shown in Fig. 5c, DEX treatment reduced the percent of PSD95+ synapses containing pCofilin-ir; although levels were lower at all time points following treatment, the 15-min time point exhibited a significant (~46 %)

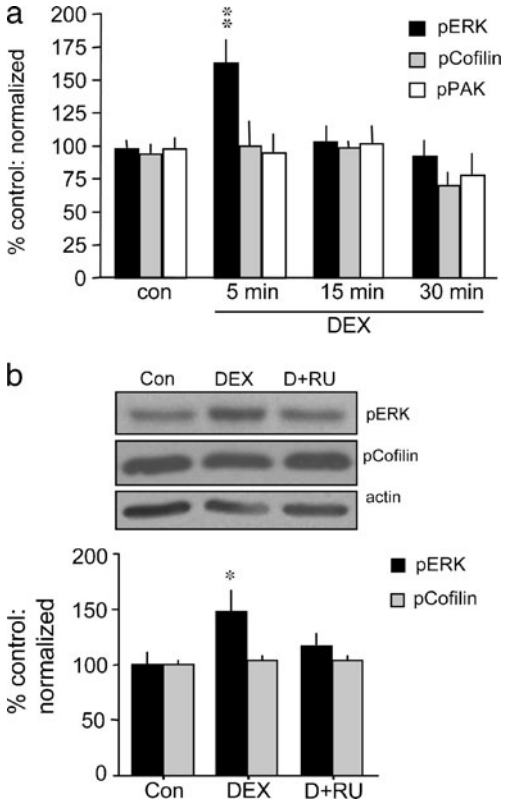

Fig. 4 DEX increases pERK1/2, but not pCofilin or pPAK, in synaptoneurosomes (SNSs). **a** Bar graph shows the effect of 5 μM DEX treatment for 5, 15, or 30 min on pERK, pCofilin, and pPAK levels: DEX increased pERK (42 kDa protein measures) at 5 min but had no effect on pCofilin or pPAK at any time point (**$p<0.001$ vs control, SNK post hoc test; $n=5$/group). **b** *Top*, representative blots of pERK (42 kDa band shown) and pCofilin immunoreactivities from control and 5 min DEX-treated SNSs. DEX increased pERK but not pCofilin levels; RU-486 blocked the DEX effect on pERK. *Bottom*, bar graph shows quantitative results for these experiments (*$p<0.01$ vs control, SNK post hoc test; $n=8$–12/group); band measures were normalized to sample actin levels from same blot and expressed as percent of respective controls

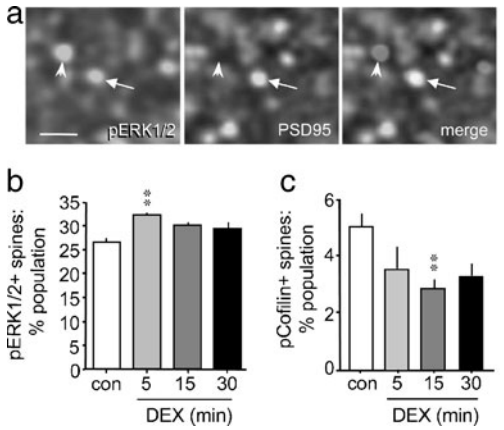

Fig. 5 DEX increases pERK1/2 and decreases pCofilin within dendritic spines. Acute hippocampal slices were prepared from adult rat, treated with 5 μM DEX for 5, 15, or 30 min and then analyzed for immunofluorescence in CA1 str. radiatum. Control (con) slices were treated with vehicle and harvested in parallel with the 30 min DEX group, as preliminary studies demonstrated no differences in labeling for control slices harvested at 5–30 min. **a** Images show immunolabeling for pERK (*left*), PSD95 (*middle*), and the two merged (*right*). The pERK1/2-ir was localized to single- (*arrowhead*) and double- (*arrow*) labeled puncta within the size constraints of synaptic elements. *Calibration bar*=2 μm. **b** Bar graph shows DEX increased numbers of pERK1/2+ PSDs within 5 min by nearly 13 % (**$p<0.01$ vs con, SNK post hoc test, $n=5$/group). **c** Quantification of double-labeled, pCofilin +/PSD95+ elements shows that DEX reduced numbers of pCofilin+ spines by 15 min (**$p<0.01$ vs con, SNK post hoc test, $n=4$–5/group). In panels **b** and **c**, values are expressed as a percent of the total PSD95+ puncta count in sample field

reduction in pCofilin-containing synapses compared to control values ($p<0.01$, SNK). Finally, it should be noted that the reduction occurs in a small population of spines (the percent of PSD95+ puncta containing pCofilin was ~5 % in control slices), and this may account for the failure to detect the effect in SNS as measured by western blotting.

Discussion

While there is evidence that glucocorticoids can elicit striking effects on spines of hippocampal CA1 neurons [11, 35], there has been little information on the degree to which the glucocorticoid receptors are present in these spines in vivo. Results of the present studies demonstrate that GRs are indeed localized to dendritic spines of adult CA1 pyramidal cells in both rat and mouse. The results of separate analyses using GR+ PSD95 double-immunolabeling and 3D reconstructions to localize GR-ir within GFP-positive dendrites and spines were complementary and showed that ~15–25 % of spines in CA1 stratum radiatum contain GR-ir, with approximately 14 % of the GR+ aggregates localized to spine heads and 11 % to spine necks. Interestingly, some GR-immunoreactive puncta were situated adjacent to the spine surface consistent with reports that GRs may be membrane bound in addition to being present within the cytoplasm [58–60]. The present results also indicate that (a) GR protein is translated in spines in response to group 1 mGluR activation and (b) spine levels of GR-ir (i.e., the volumes of GR+ aggregates) are reduced in mice lacking the translational regulator FMRP. Both findings are consistent with a recent report indicating that GRα mRNA is a cargo of FMRP [12], a protein that transports mRNA into dendrites and spines and regulates local protein synthesis upon group 1 mGluR activation ([44] for review). Thus, the collective findings indicate that GR protein is synthesized in spines and this occurs, in part, via an FMRP-dependent local protein synthesis mechanism. As mGluR-dependent local protein synthesis occurs within minutes [61], such a mechanism could allow for rapid changes in spine GR levels and more dynamic responsivity to glucocorticoids.

Glucocorticoids influence signaling to the actin cytoskeleton in a number of cell types by acting on the small Rho

GTPases. For example, prolonged (3 days) treatment of podocytes with the specific GR agonist DEX selectively increases levels of activated (GTP-bound) RhoA, but not Rac [21]; the latter result is consistent with our finding that DEX has no effect on phosphorylation of PAK, a downstream effector of Rac, in either the hippocampal slice cultures or synaptoneurosome preparations. Further, prolonged DEX treatment of Con8 (mammary epithelial tumor) cells is reported to influence the activity of RhoA effectors ROCK 1 and 2 [22], which activate LIM kinase leading to cofilin phosphorylation. Cofilin acts to sever and depolymerize actin but upon phosphorylation becomes deactivated, thus promoting actin polymerization [50]. In line with these observations, we find that acute DEX treatment causes marked and rapid (within 30 min) increases in total pCofilin levels in hippocampal slice cultures as determined by western blot analysis of whole tissue homogenates. These results demonstrate that, in general, glucocorticoids engage the RhoA>> cofilin signaling pathway involved in regulating actin polymerization but do not provide information on the hippocampal region, or cellular compartment, of the DEX-induced pCofilin increases; thus, increases could reflect broadly distributed elevations in phospho-protein levels across different hippocampal strata, or effects limited to a subfield or specific cell type. Regarding the later point, excess exposure to glucocorticoids over days has pronounced structural effects on hippocampal CA3 neurons including reduced dendritic branching and neuronal loss, with little-to-no effects on CA1 neurons [62–64]. It is possible then that the DEX-induced increases in total pCofilin content in hippocampal slice cultures reflect selective actions on field CA3 and, in particular, a compensatory mechanism promoting actin polymerization for cell structure maintenance in response to short-term glucocorticoid exposure. Further studies are needed to determine if this is the case, and if DEX effects on pCofilin are greater in cells that are particularly vulnerable to excessive glucocorticoids.

Semi-chronic stress and/or elevations in glucocorticoids have been shown to increase levels of pERK1/2 via activation of the Rho GTPases Ras/Raf [65]; pERK1/2 contributes to F-actin stabilization and arrangement. In particular, Lee et al. [66] found that stress (2 h/day for 7 days) increased total pERK1/2 levels in several rat brain regions including hippocampus; similarly Yang et al. [65] found increases following 1 h of tail-shock stress. Munhoz et al. [67] showed that in rat several days of elevated circulating corticosterone, equivalent to effects of a moderate stressor, increased ERK1/2 phosphorylation in neocortex and hippocampus. In accord with these reports, we found that DEX treatment of hippocampal slice cultures increased total pERK1/2 content. Importantly, the present data also demonstrate that these effects are rapid, occurring within minutes.

Glucocorticoid receptor agonists have rapid and profound effects on dendritic spine density and morphology. DEX induces a rapid (within 1 h) increase in spine density on secondary dendrites of hippocampal CA1 pyramidal neurons, with select increases in thin and mushroom type spines [11]. This effect is not protein synthesis dependent but is blocked by both the specific GR inhibitor RU-486 and NMDA receptor antagonism, supporting the conclusion that effects on spine morphology are non-genomic and mediated by local GR functions. Thus, glucocorticoids can clearly influence both spine morphology and number, but the question remained as to how this occurs beyond the potential involvement of NMDA receptors. With this in mind, the present studies first

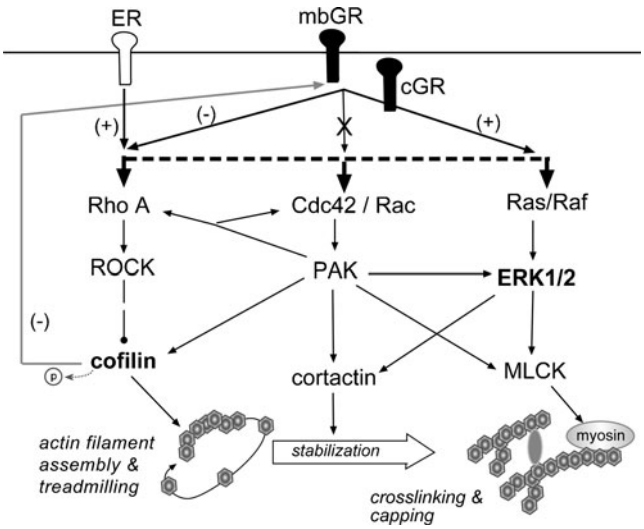

Fig. 6 Schematic showing actin cytoskeleton signaling pathways in adult hippocampal spines (see [19]) and the proposed mechanisms by which the glucocorticoid receptor (GR) affects actin assembly and stabilization. The GR is represented as being both membrane bound (mb) and in the cytoplasm (c; see [58]). Shown are the major Rho GTPase signaling pathways involved in regulating spine F-actin assembly and stabilization. Activation of RhoA leads to the phosphorylation of cofilin which blocks its constitutive F-actin severing activities thus promoting filament assembly (i.e., polymerization). Newly polymerized actin undergoes "treadmilling," a process whereby actin monomers are continuously removed from one end and added to the other end of the filaments, prior to stabilization by processes that involve activation of Cdc42/Rac and Ras/Raf pathways. The present results demonstrate that in spines DEX-induced GR activation reduces levels of phosphorylated cofilin, which is downstream of the Rho GTPase RhoA and it's effector ROCK; the exact mechanism by which this negative (−) action occurs is not known, but could arise through inhibition of RhoA or its downstream effectors, or activation of phosphatases (not shown). By comparison, the estrogen receptor (ER) markedly facilitates (+) activation of RhoA and increases phosphorylated cofilin levels and actin polymerization in adult hippocampal spines [68]. Recent work showing that dephosphorylation of cofilin reduces GR activation [70] also is illustrated (*gray pathway*), although this negative feedback mechanism has not been confirmed in spines. GR activation also increases spine levels of phosphorylated ERK1/2, possibly via the activation of Rho GTPases Ras/Raf, which can affect both actin stabilization via cortactin and actin rearrangement via myosin light chain kinase (MLCK) and its effects on myosin. Activation of GR does not increase pPAK suggesting that the receptor does not influence the Cdc42/Rac> PAK pathway

determined the degree to which GRs are present in hippocampal CA1 spines and then demonstrated that synaptic levels of this receptor are regulated by group 1 mGluR- and FMRP-dependent mechanisms. Thus, in the hippocampal CA1 field, GRs are positioned to rapidly influence spine populations, a process that we posited might occur through influences on actin regulatory signaling pathways shown to effect and stabilize spine cytoskeletal changes in this field (Fig. 6) [19].

The present results confirm that acting through the GRs, DEX modulates spine actin regulatory signaling. Immunohistochemical analyses showed that acute DEX treatment of adult hippocampal slices significantly reduced the number of spines containing pCofilin-ir in CA1 str. radiatum. This finding was not evident with western blot analysis of whole slice homogenates (which showed an increase in total pCofilin content), thereby suggesting the intriguing possibility that glucocorticoid effects on F-actin may differ across subfields and/or cellular compartments; reduced pCofilin in field CA1 spines would promote local actin severing whereas elevated pCofilin elsewhere would promote actin polymerization. It is interesting to note that unlike the effect of DEX, LTP-inducing stimulation increases numbers of hippocampal spines containing pCofilin in field CA1 [19, 27, 68]. The LTP studies have further shown that activity-induced increases in cofilin phosphorylation are mediated by activation of RhoA and ROCK (Fig. 6) [19]. Taken together, the present results suggest that glucocorticoids could modulate the responsivity of the RhoA>> cofilin pathway engaged by other receptors, including those that facilitate LTP, to influence spine F-actin polymerization. Activation of the estrogen receptor increases actin polymerization in adult hippocampal spines through activation of RhoA>> cofilin signaling (Fig. 6) and facilitates LTP [68, 69]. The GRs could modulate the effects of estrogen receptors on spine actin by depressing pCofilin content. While the mechanism(s) through which the glucocorticoids reduce cofilin phosphorylation in spines remains to be determined, it could involve either inhibition of RhoA or ROCK activity or activation of phosphatases. Finally, recent work suggests that the phosphorylation state of cofilin can reciprocally affect GR activation; work in HeLA cells demonstrates that cofilin in its unphosphorylated state inhibits GR activation thus providing a negative feedback loop to regulate local GR signaling [70]. Whether this mechanism also is present in spines remains to be determined.

The second spine actin regulatory pathway affected by glucocorticoids involves ERK1/2. Like Rac> PAK signaling [71], pERK1/2 activates cortactin [51], an actin binding protein shown to stabilize F-actin [53] (Fig. 6). Another target of pERK1/2 is myosin light chain kinase (MLCK) which activates myosin thereby promoting its interaction with F-actin and leading to actin rearrangement [72]. DEX treatment of synaptoneurosomes caused marked (~50 %) increases in phosphorylation of ERK1/2 within minutes, and this effect was blocked by RU-486. Thus, glucocorticoids acting through GRs facilitate the activity of a protein that works to both stabilize and rearrange spine F-actin; such actions are likely to promote spinogenesis, and are consistent with the observation that GRs play a role in cortical spine formation but not elimination [36]. However, because DEX had opposite effects on ERK1/2 and cofilin phosphorylation in spines, it is possible that the overall effect of glucocorticoids at synapses could favor less synaptic plasticity (i.e., less polymerization relative to stabilization of actin filaments). While some have found that high levels of glucocorticoids inhibit hippocampal field CA1 LTP and other forms of potentiation ([37]; see [38] for review), this idea needs further testing to determine if (a) spine F-actin is more stable and less vulnerable to disruption following glucocorticoid treatment and (b) the effects described here, elicited by high stress levels of glucocorticoids, are also obtained with lower doses. The latter point is of particular interest because low levels of stress are generally observed to facilitate learning [73–76]. Therefore, it will be important to determine if low doses of glucocorticoids or low levels of stress tip the balance of spine actin regulatory signaling toward favoring actin polymerization, a critical first step in synaptic plasticity. Finally, as the mineralocorticoid receptor has been reported to engage the postsynaptic ERK1/2 pathway in CA1 pyramidal cells [57], future studies are needed to address the degree to which the glucocorticoid and mineralocorticoid receptors influence this signaling pathway, and the consequence of this convergent regulation on spine actin dynamics.

Acknowledgments This work was supported by the National Institute of Mental Health (MH082042 to C.G. and J.L. and FMH095432A to R.S.) and the National Institute of General Medical Sciences (T32-GM0862 to R.S.). The authors would like to thank Dr. Jihua Liu, Yue Qin Yao, and Adam Katz for invaluable technical support, Elliot Handler for help with microscopy, Dr. Gary Lynch for his intellectual contributions and help with the schematic, and Dr. Tallie Z. Baram for valuable comments and discussion.

Conflict of Interest The authors declare that they have no conflict of interest.

References

1. Romeo RD, Waters EM, McEwen BS (2004) Steroid-induced hippocampal synaptic plasticity: sex differences and similarities. Neuron Glia Biol 1:219–229
2. Tata DA, Anderson BJ (2010) The effects of chronic glucocorticoid exposure on dendritic length, synapse numbers and glial volume in animal models: implications for hippocampal volume reductions in depression. Physiol Behav 99:186–193
3. Chaouloff F, Groc L (2011) Temporal modulation of hippocampal excitatory transmission by corticosteroids and stress. Front Neuroendocrinol 32:25–42

4. Haller J, Mikics E, Makara GB (2008) The effects of non-genomic glucocorticoid mechanisms on bodily functions and the central neural system. A critical evaluation of findings. Front Neuroendocrinol 29:273–291
5. Evanson NK, Herman J, P., Sakai RR, Krause EG (2010) Non-genomic actions of adrenal steroids in the central nervous system. J Neuroendocrinol. 846–861
6. Ffrench-Mullen JM (1995) Cortisol inhibition of calcium currents in guinea pig hippocampal CA1 neurons via G-protein-coupled activation of protein kinase C. J Neurosci 15:903–911
7. Karst H, Berger S, Turiault M, Tronche F, Schütz G, Joëls M (2005) Mineralocorticoid receptors are indispensable for nongenomic modulation of hippocampal glutamate transmission by corticosterone. Proc Natl Acad Sci USA 102:19204–19207
8. Qi AQ, Qiu J, Xiao L, Chen YZ (2005) Rapid activation of JNK and p38 by glucocorticoids in primary cultured hippocampal cells. J Neurosci Res 80:510–517
9. Tasker JG, Di S, Malcher-Lopes R (2006) Minireview: rapid glucocorticoid signaling via membrane-associated receptors. Endocrinology 147:5549–5556
10. Johnson LR, Farb C, Morrison JH, McEwen BS, LeDoux JE (2005) Localization of glucocorticoid receptors at postsynaptic membranes in the lateral amygdala. Neuroscience 136:289–299
11. Komatsuzaki Y, Murakami G, Tsurugizawa T, Mukai H, Tanabe N, Mitsuhashi K, Kawata M, Kimoto T, Ooishi Y, Kawato S (2005) Rapid spinogenesis of pyramidal neurons induced by activation of glucocorticoid receptors in adult male rat hippocampus. Biochem Biophys Res Commun 335:1002–1007
12. Miyashiro KY, Beckel-Mitchener A, Purk TP, Becker KG, Barret T, Liu L, Carbonetto S, Weiler IJ, Greenough WT, Eberwine J (2003) RNA cargoes associating with FMRP reveal deficits in cellular functioning in Fmr1 null mice. Neuron 37:417–431
13. Krugers HJ, Hoogenraad CC, Groc L (2010) Stress hormones and AMPA receptor trafficking in synaptic plasticity and memory. Nat Rev Neurosci 11:675–681
14. Pavlides C, Watanabe Y, Magariños AM, McEwen BS (1995) Opposing roles of type I and type II adrenal steroid receptors in hippocampal long-term potentiation. Neuroscience 68:387–394
15. Alfarez DN, Wiegert O, Joëls M, Krugers HJ (2002) Corticosterone and stress reduce synaptic potentiation in mouse hippocampal slices with mild stimulation. Neuroscience 115:1119–1126
16. Maggio N, Segal M (2007) Striking variations in corticosteroid modulation of long-term potentiation along the septotemporal axis of the hippocampus. J Neurosci 27:5757–5765
17. Wiegert O, Pu Z, Shor S, Joëls M, Krugers HJ (2005) Glucocorticoid receptor activation selectively hampers N-methyl-D-aspartate receptor dependent hippocampal synaptic plasticity in vitro. Neuroscience 135:403–411
18. Lynch G, Rex CS, Chen LY, Gall CM (2008) The substrates of memory: defects, treatments, and enhancement. Eur J Pharmacol 585:2–13
19. Rex CS, Chen LY, Sharma A, Liu J, Babayan AH, Gall CM, Lynch G (2009) Different Rho GTPase-dependent signaling pathways initiate sequential steps in the consolidation of long-term potentiation. J Cell Biol 186:85–97
20. Krucker T, Siggins GR, Halpain S (2000) Dynamic actin filaments are required for stable long-term potentiation (LTP) in area CA1 of the hippocampus. Proc Natl Acad Sci USA 97:6856–6861
21. Ransom RF, Lam NG, Hallett MA, Atkinson SJ, Smoyer WE (2005) Glucocorticoids protect and enhance recovery of cultured murine podocytes via actin filament stabilization. Kidney Int 68:2473–2483
22. Rubenstein NM, Callahan JA, Lo DH, Firestone GL (2007) Selective glucocorticoid control of Rho kinase isoforms regulate cell-cell interactions. Biochem Biophys Res Commun 354:603–607
23. Filla MS, Schwinn MK, Nosie AK, Clark RW, Peters DM (2011) Dexamethasone-associated cross-linked actin network formation in human trabecular meshwork cells involves β3 integrin signaling. Invest Ophthalmol Vis Sci 52:2952–2959
24. Bakker CE, Verheij C, Willemsen R, Vanderhelm R, Oerlemans F, Vermey M, Bygrave A, Hoogeveen AT, Oostra BA, Reyniers E, Deboulle K, Dhooge R, Cras P, Vanvelzen D, Nagels G, Martin JJ, Dedyn PP, Darby JK, Willems PJ, Consortium TD-BFX (1994) Fmr1 knockout mice: a model to study fragile x mental retardation. The Dutch-Belgium Fragile X Consortium. Cell 78:23–33
25. Feng G, Mellor RH, Bernstein M, Keller-Peck C, Nguyen QT, Wallace M, Nerbonne JM, Lichtman JW, Sanes JR (2000) Imaging neuronal subsets in transgenic mice expressing multiple spectral variants of GFP. Neuron 28:41–51
26. D'Agostino J, Vaeth GF, Henning SJ (1982) Diurnal rhythm of total and free concentrations of serum corticosterone in the rat. Acta Endocrinol (Copenh) 100:85–90
27. Chen LY, Rex CS, Casale M, Gall CM, Lynch G (2007) Changes in synaptic morphology accompany actin signaling during LTP. J Neurosci 27:5363–5372
28. Sarabdjitsingh RA, Meijer OC, de Kloet ER (2010) Specificity of glucocorticoid receptor primary antibodies for analysis of receptor localization patterns in cultured cells in hippocampus. Brain Res 1331:1–11
29. Bickel PE, Scherer PE, Schnitzer JE, Oh P, Lisanti MP, Lodish HF (1997) Flotillin and epidermal surface antigen define a new family of caveolae-associated integral membrane proteins. J Biol Chem 272:13793–13802
30. Chen LY, Rex CS, Babayan AH, Kramár EA, Lynch G, Gall CM, Lauterborn JC (2010) Physiological activation of synaptic Rac> PAK (p-21 activated kinase) signaling is defective in a mouse model of fragile X syndrome. J Neurosci 30:10977–10984
31. Chen L, Rex C, Sanaiha Y, Lynch G, Gall C (2010) Learning induces neurotrophin signaling at hippocampal synapses. Proc Natl Acad Sci USA 107:7030–7035
32. Chen LY, Rex CS, Pham DT, Lynch G, Gall CM (2010) BDNF signaling during learning is regionally differentiated within hippocampus. J Neurosci 30:15097–15101
33. Rex CS, Gavin CF, Rubio MD, Kramar EA, Chen LY, Jia Y, Huganir RL, Muzyczka N, Gall CM, Miller CA, Lynch G, Rumbaugh G (2010) Myosin IIb regulates actin dynamics during synaptic plasticity and memory formation. Neuron 67:603–617
34. Lauterborn JC, Pineda EA, Chen LY, Ramirez EA, Lynch G, Gall CM (2009) Ampakines cause sustained increases in brain-derived neurotrophic factor signaling at excitatory synapses without changes in AMPA receptor subunit expression. Neuroscience 159:283–295
35. Morales-Medina JC, Sanchez F, Flores G, Dumont Y, Quirion R (2009) Morphological reorganization after repeated corticosterone administration in the hippocampus, nucleus accumbens and amygdala in the rat. J Chem Neuroanat 38:266–272
36. Liston C, Gan WB (2011) Glucocorticoids are critical regulators of dendritic spine development and plasticity in vivo. Proc Natl Acad Sci USA 108:16074–16079
37. Diamond DM, Bennett MC, Fleshner M, Rose GM (1992) Inverted-U relationship between the level of peripheral corticosterone and the magnitude of hippocampal primed burst potentiation. Hippocampus 2:421–430
38. Joëls M, Krugers HJ (2007) LTP after stress: up or down? Neural Plast 2007:93202–93208
39. Bernard-Trifilo JA, Kramár EA, Torp R, Lin CY, Pineda EA, Lynch G, Gall CM (2005) Integrin signaling cascades are operational in adult hippocampal synapses and modulate NMDA receptor physiology. J Neurochem 93:834–849
40. Megías M, Emri Z, Freund TF, Gulyás AI (2001) Total number and distribution of inhibitory and excitatory synapses on hippocampal CA1 pyramidal cells. Neuroscience 102:527–540
41. Aoki C, Miko I, Oviedo H, Mikeladze-Dvali T, Alexandre L, Sweeney N, Bredt DS (2001) Electron microscopic immunocytochemical

detection of PSD-95, PSD-93, SAP-102, and SAP-97 at postsynaptic, presynaptic, and nonsynaptic sites of adult and neonatal rat visual cortex. Synapse 40:239–257
42. Hunt C, Schenker L, Kennedy M (1996) PSD-95 is associated with the postsynaptic density and not with the presynaptic membrane at forebrain synapses. J Neurosci 16:1380–1388
43. Sans N, Petralia R, Wang Y, Jn B, Hell J, Wenthold R (2000) A developmental change in NMDA receptor-associated proteins at hippocampal synapses. J Neurosci 20:1260–1271
44. Ronesi JA, Huber KM (2008) Metabotropic glutamate receptors and fragile x mental retardation protein: partners in translational regulation at the synapse. Sci Signal 1:pe6
45. Dictenberg JB, Swanger SA, Antar LN, Singer RH, Bassell GJ (2008) A direct role for FMRP in activity-dependent dendritic mRNA transport links filopodial-spine morphogenesis to fragile X syndrome. Dev Cell 14:926–939
46. Kao DI, Aldridge GM, Weiler IJ, Greenough WT (2010) Altered mRNA transport, docking, and protein translation in neurons lacking fragile X mental retardation protein. Proc Natl Acad Sci USA 107:15601–15606
47. Todd PK, Mack KJ, Malter JS (2003) The fragile X mental retardation protein is required for type-I metabotropic glutamate receptor-dependent translation of PSD-95. Proc Natl Acad Sci USA 100:14374–14378
48. Kramár EA, Lin B, Rex CS, Gall CM, Lynch G (2006) Integrin-driven actin polymerization consolidates long-term potentiation. Proc Natl Acad Sci USA 103:5579–5584
49. Kim JJ, Diamond DM (2002) The stressed hippocampus, synaptic plasticity and lost memories. Nat Rev Neurosci 3:453–462
50. Bamburg JR, McGough A, Ono S (1999) Putting a new twist on actin: ADF/cofilins modulate actin dynamics. Trends Cell Biol 9:364–370
51. Martinez-Quiles N, Ho HY, Kirschner MW, Ramesh N, Geha RS (2004) Erk/Src phosphorylation of cortactin acts as a switch on-switch off mechanism that controls its ability to activate N-WASP. Mol Cell Biol 24:5269–5280
52. Mullins RD, Heuser JA, Pollard TD (1998) The interaction of Arp2/3 complex with actin: nucleation, high affinity pointed end capping, and formation of branching networks of filaments. Proc Natl Acad Sci USA 95:6181–6186
53. Weaver AM, Karginov AV, Kinley AW, Weed SA, Li Y, Parsons JT, Cooper JA (2001) Cortactin promotes and stabilizes Arp2/3-induced actin filament network formation. Curr Biol 11:370–374
54. Wang YF, Hatton GI (2007) Interaction of extracellular signal-regulated protein kinase 1/2 with actin cytoskeleton in supraoptic oxytocin neurons and astrocytes: role in burst firing. J Neurosci 27:13822–13834
55. Lynch MA (2004) Long-term potentiation and memory. Physiol Rev 84:87–136
56. Alonso M, Medina JH, Pozzo-Miller L (2004) ERK1/2 activation is necessary for BDNF to increase dendritic spine density in hippocampal CA1 pyramidal neurons. Learn Mem 11:172–178
57. Olijslagers JE, de Kloet ER, Elgersma Y, van Woerden GM, Joëls M, Karst H (2008) Rapid changes in hippocampal CA1 pyramidal cell function via pre- as well as postsynaptic membrane mineralocorticoid receptors. Eur J Neurosci 27:2542–2550
58. Hill MN, McEwen BS (2009) Endocannabinoids: The silent partner of glucocorticoids in the synapse. Proc Natl Acad Sci USA 106:4579–4580
59. Barsegyan A, Mackenzie SM, Kurose BD, McGaugh JL, Roozendaal B (2010) Glucocorticoids in the prefrontal cortex enhance memory consolidation and impair working memory by a common neural mechanism. Proc Natl Acad Sci USA 107:16655–16660
60. Schmidt KL, Malisch JL, Breuner CW, Soma KK (2010) Corticosterone and cortisol binding sites in plasma, immune organs and brain of developing zebra finches: intracellular and membrane-associated receptors. Brain Behav Immun 24:908–918
61. Weiler IJ, Greenough WT (1993) Metabotropic glutamate receptors trigger postsynaptic protein synthesis. Proc Natl Acad Sci USA 90:7168–7171
62. Woolley CA, Gould E, McEwen BS (1990) Exposure to excess glucocorticoids alters dendritic morphology of adult hippocampal pyramidal neurons. Brain Res 531:225–231
63. Magarinos AM, McEwen BS (1995) Stress-induced atrophy of apical dendrites of hippocampal CA3c neurons: comparison of stressors. Neuroscience 69:83–88
64. Sousa N, Paula-Barbosa MM, Almeida OF (1999) Ligand and subfield specificity of corticoid-induced neuronal loss in the rat hippocampal formation. Neuroscience 89:1079–1087
65. Yang CH, Huang CC, Hsu KS (2004) Behavioral stress modifies hippocampal synaptic plasticity through corticosterone-induced sustained extracellular signal-regulated kinase/mitogen-activated protein kinase activation. J Neurosci 24:11029–11034
66. Lee SY, Kang JS, Song GY, Myung CS (2006) Stress induces the expression of heterotrimeric G protein beta subunits and the phosphorylation of PKB/Akt and ERK1/2 in rat brain. Neurosci Res 56:180–192
67. Munhoz CD, Sorrells SF, Caso JR, Scavone C, Sapolsky RM (2010) Glucocorticoids exacerbate lipopolysaccharide-induced signaling in the frontal cortex and hippocampus in a dose-dependent manner. J Neurosci 30:13690–13698
68. Kramár EA, Chen LY, Brandon NJ, Rex CS, Liu F, Gall CM, Lynch G (2009) Cytoskeletal changes underlie estrogen's acute effects on synaptic transmission and plasticity. J Neurosci 29:12982–12993
69. Kramár E, Chen L, Lauterborn J, Simmons D, Gall C, Lynch G (2010) BDNF and BDNF upregulation restores synaptic plasticity in middle-aged ovariectomized rats in Society for Neuroscience. 2010 Neuroscience Meeting Planner, San Diego
70. Rüegg J, Holsboer F, Turck C, Rein T (2004) Cofilin 1 is revealed as an inhibitor of glucocorticoid receptor by analysis of hormone-resistant cells. Mol Cell Biol 24:9371–9382
71. Webb BA, Zhou S, Eves R, Shen L, Jia L, Mak AS (2006) Phosphorylation of cortactin by p21-activated kinase. Arch Biochem Biophys 456:183–193
72. Inoue Y, Tsuda S, Nakagawa K, Hojo M, Adachi T (2011) Modeling myosin-dependent rearrangement and force generation in an actomyosin network. J Theor Biol 281:65–73
73. Oitzl MS, de Kloet ER (1992) Selective corticosteroid antagonists modulate specific aspects of spatial orientation learning. Behav Neurosci 106:62–71
74. Shors TJ, Weiss C, Thompson RF (1992) Stress-induced facilitation of classical conditioning. Science 257:537–539
75. Sandi C, Rose SP (1994) Corticosterone enhances long-term retention in one-day-old chicks trained in a weak passive avoidance learning paradigm. Brain Res 647:106–112
76. Sandi C, Loscertales M, Guaza C (1997) Experience-dependent facilitating effect of corticosterone on spatial memory formation in the water maze. Eur J Neurosci 9:637–642